Journal of Alloys and Compounds 509 (2011) 3547–3552

Contents lists available at ScienceDirect

Journal of Alloys and Compounds

journal homepage: www.elsevier.com/locate/jallcom

Dielectric properties of $PbTiO_3$/ZnO ceramic nanocomposites obtained by solid-state reaction method

R. Wongmaneerung[a,*], S. Choopan[b], R. Yimnirun[c], S. Ananta[b]

[a] Materials Science Program, Faculty of Science, Maejo University, Chiang Mai 50290, Thailand
[b] Department of Physics and Materials Science, Faculty of Science, Chiang Mai University, Chiang Mai 50200, Thailand
[c] School of Physics, Institute of Science, Suranaree University of Technology, Nakhon Ratchasima 30000, Thailand

ARTICLE INFO

Article history:
Received 30 July 2010
Received in revised form 3 December 2010
Accepted 3 December 2010
Available online 10 December 2010

Keywords:
Ferroelectric
Lead titanate
Zinc oxide
Dielectric response
Nanocomposites

ABSTRACT

In this paper, we report on the dielectric properties of $PbTiO_3$/ZnO ceramic nanocomposites prepared by a conventional solid-state reaction method with improvement in densification by the addition of ZnO nanowhiskers. Phase formation, densification, microstructure and dielectric properties of the composites were investigated as a function of the content of ZnO nanowhiskers. Densification behavior of the ceramic nanocomposites was significantly enhanced, as compared to pure $PbTiO_3$ ceramics. Moreover, the dielectric constant of the composites was higher than that of the pure $PbTiO_3$ ceramics.

1. Introduction

Dense perovskite lead titanate ($PbTiO_3$ or PT) based ceramics are known to exhibit excellent dielectric, piezoelectric and pyroelectric properties for use in electronic and electro-optic devices at high temperatures and high frequencies [1]. However, it is well known that pure PT ceramics are difficult to obtain because they break up into powders when they are cooled down through the Curie point, due to the large distortion of the tetragonal phase at room temperature (which is characterized by a c/a ratio of ~1.06) [2,3]. Therefore, dielectric properties of PT ceramics are only available for porous and doped samples. Also, such samples usually have very high conductivity at elevated temperatures.

The concept of a functionally graded material has been used to overcome the mechanical problems. Piezoelectric ceramic/ceramic functionally graded materials have been studied in order to reduce the stress concentration in the actuators [4,5]. However, problems still exist with the thermal expansion mismatch. Several approaches to improve the mechanical strength of the composites by incorporating polymers, metals, fibers or whiskers have been investigated [6–10].

In an attempt to improve the dielectric properties of ferroelectric ceramics, ceramic nanocomposites consisting of two or more components with different macroscopic properties have shown promise due to the improvement in both physical and mechanical properties. In the past few years, additional attempts have been carried out by the addition of oxide particles such as ZrO_2 and MgO [11–13]. Moreover, piezoelectric nanocomposites embedded with ZnO whiskers, such as PZT/ZnO composites, have been prepared through a normal sintering process in air. The composites not only retained good piezoelectric properties, but also exhibited excellent and significantly improved mechanical properties. A few studies have been conducted on ferroelectric matrix/metal nanodispersoid [14] and non-ferroelectric matrix/ferroelectric nanodispersoid [15]. PT ceramic-based composites have recently been developed to improve the mechanical and dielectric properties [16,17]. Silicon carbide (SiC) nanofibers and PT nanopowders have been employed as the reinforcement in the composites because of their ability to resist crack growth [18]. However, the addition of SiC nanofibers leads to reduced dielectric constant. ZnO has received much attention as a reinforced composite material due to its high-temperature strength and excellent chemical stability [19]. No work on PT/ZnO composites has yet been reported. In this paper, PT ceramics doped with ZnO nanowhiskers (0.1–5.0 wt%) were fabricated by a conventional solid-state reaction method. Effects of the ZnO nanowhiskers on the microstructure and dielectric properties of the composites were studied and discussed.

* Corresponding author. Tel.: +66 53 873515.
E-mail address: re_nok@yahoo.com (R. Wongmaneerung).

0925-8388/$ – see front matter © 2010 Elsevier B.V. All rights reserved.
doi:10.1016/j.jallcom.2010.12.024

Table 1
Physical properties of PT/ZnO composites sintered at 1200 °C for 2 h.

ZnO nanowhisker (wt%)	Perovskite phase[a] (%)	Tetragonality (c/a)	Relative density (%)	Grain size[b] (mean) (μm)
0.0	100.00	1.063	94	20.0–65.0 (36)
0.1	100.00	1.061	96	0.5–1.7 (0.8)
0.5	100.00	1.061	98	0.3–1.3 (0.7)
1.0	100.00	1.060	98	0.3–1.0 (0.7)
3.0	98.56	1.061	97	0.5–2.2 (1.6)
5.0	95.23	1.060	98	0.7–3.7 (2.0)

[a] The estimated precision of the perovskite phase is ±0.1%.
[b] The estimated precision of the grain size is ±10%.

2. Experimental

PT/ZnO ceramic nanocomposites were prepared using the conventional solid-state reaction and subsequent pressureless sintering process. Commercially available powders of PbO (Fluka, >99.9% purity) and TiO_2 (Aldrich, >99.9% purity) were used as raw materials to produce PT powders. Composites were made with the synthesized PT powders (average particle size ~1–5 μm) and ZnO nanowhiskers [20] (average diameter ~0.4–2 μm and ~12–36 μm length), as shown in Fig. 1. Different amounts (0.1–5.0 wt%) of ZnO nanowhiskers were ultrasonically dispersed in ethanol for 10 min before vibro-mixing with the PT powders. The powder mixtures were formed into pellets by adding 3 wt% polyvinyl alcohol (PVA) binder, prior to pressing in a uniaxial press at 100 MPa. For sintering, the pellets were placed in a closed alumina crucible with an atmosphere powder of identical chemical composition [16,17]. The PVA binder was burnt out at 550 °C. Samples were sintered at 1200 °C for 2 h at heating/cooling rates of 5 °C/min.

Densities of the sintered samples were measured by the Archimedes method. Phase analysis was performed by X-ray diffraction (XRD) (Siemens-D500). Tetragonality factors of the ceramic nanocomposites were calculated from the XRD patterns [21]. Microstructures of the samples were characterized using a scanning electron microscope (SEM) (JEOL JSM-840A). Grain sizes of the sintered ceramics were measured by employing the linear intercept method. In order to evaluate dielectric properties, dense ceramic nanocomposites were polished to form flat and parallel faces. The samples were coated with silver paste electrode which was fired on both sides of the samples at 550 °C for 1 h. Dielectric measurement of the sintered ceramics was performed with an LCR meter (HIOKI 3532-50). All measurements were conducted over a frequency range from 1 to 5 MHz and a temperature range from 550 °C to 25 °C.

Table 2
Dielectric properties of PT/ZnO composites measured at 1 MHz.

ZnO nanowhisker (wt%)	T_C (°C)	$\varepsilon_{25\,°C}$	tan $\delta_{25\,°C}$	$\varepsilon_{r,max}$	tan δ_{max}
0.0	482	243	0.02	7680	1.07
0.1	468	350	0.06	11,406	0.80
0.5	465	415	0.01	11,050	1.40
1.0	478	400	0.09	9696	1.18

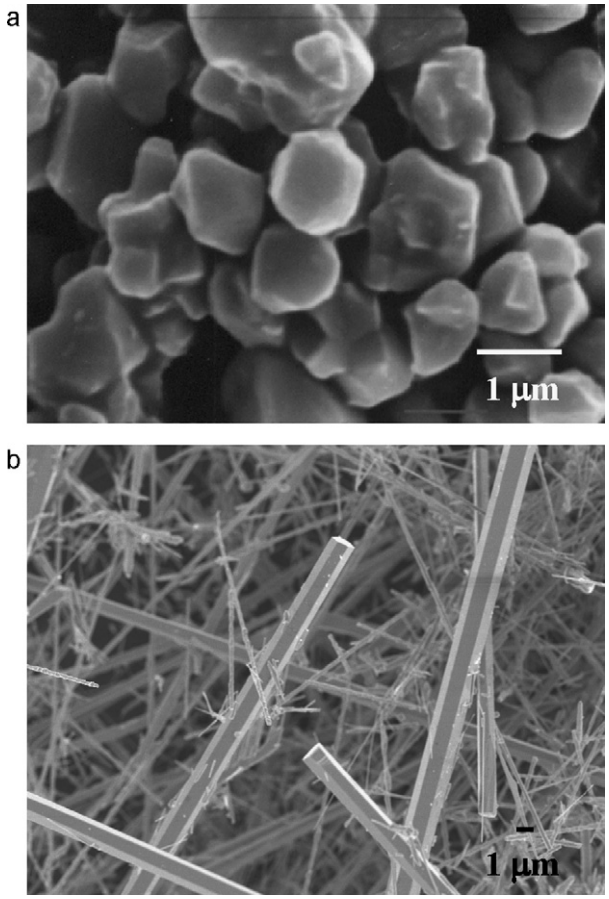

Fig. 1. SEM micrographs of (a) PT powders and (b) ZnO nanowhiskers.

3. Results and discussion

XRD patterns of monolithic PT and the PT/ZnO ceramic nanocomposites with 0.1, 0.5, 1.0, 3.0 and 5.0 wt% ZnO are shown in Fig. 2. In general, perovskite as a major PT phase is observable in all samples. No measurable change in d-spacing for the samples containing different ZnO contents was observed. All the peaks are ascribed to tetragonal $PbTiO_3$ (JCPDS file no. 6-452) [22]. Diffraction peaks of ZnO in the nanocomposites are not detectable probably because its amount was less than the XRD detection limits. However, when the content of ZnO nanowhiskers was more than 3.0 wt%, a considerable amount of Zn_2TiO_4 (▼) [23] was formed. This indicates that an evident chemical reaction occurred between PT and ZnO nanowhiskers. In the case of PZT/ZnO nanocomposites [13], it was shown that ZnO nanowhiskers were chemically inert to PZT at 1100 °C. In this work, ZnO nanowhiskers might act as a sin-

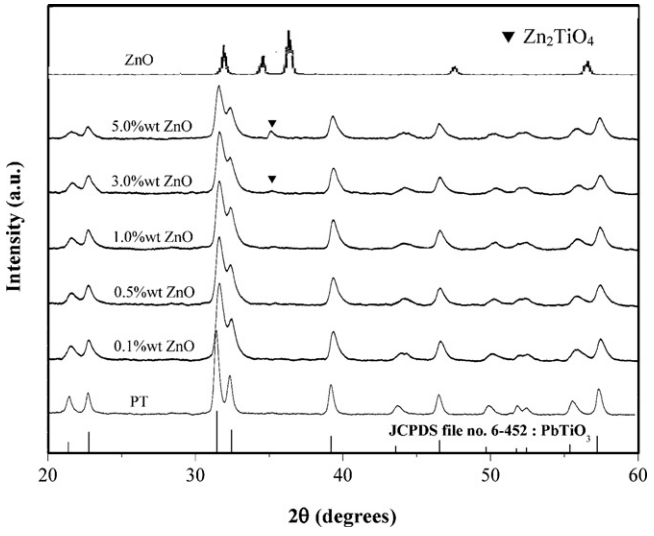

Fig. 2. XRD patterns of monolithic PT and PT/ZnO ceramics sintered at 1200 °C for 2 h.

tering aid so that samples with high ZnO contents (3.0 and 5.0 wt%) could be sintered at temperatures lower than 1200 °C. The presence of the secondary phase could be attributed to the high sintering temperature and a small degree of lead losses [24]. Moreover, by comparing these results with our previous work [17], it is found that SiC nanofibers are chemically inert to PT at identical sintering conditions.

Densities and tetragonality factors of the samples are listed in Table 1. The density values increased slightly with increasing content of ZnO nanowhiskers, from 0 to 0.5 wt%. Higher content of ZnO did not lead to further increase in density. Furthermore, the formation of oxygen vacancies due to Zn^{2+} ion substitution in perovskite structure is considered to be another reason for the sintering behavior of PT/ZnO nanocomposites [25]. Thus, the assumption that

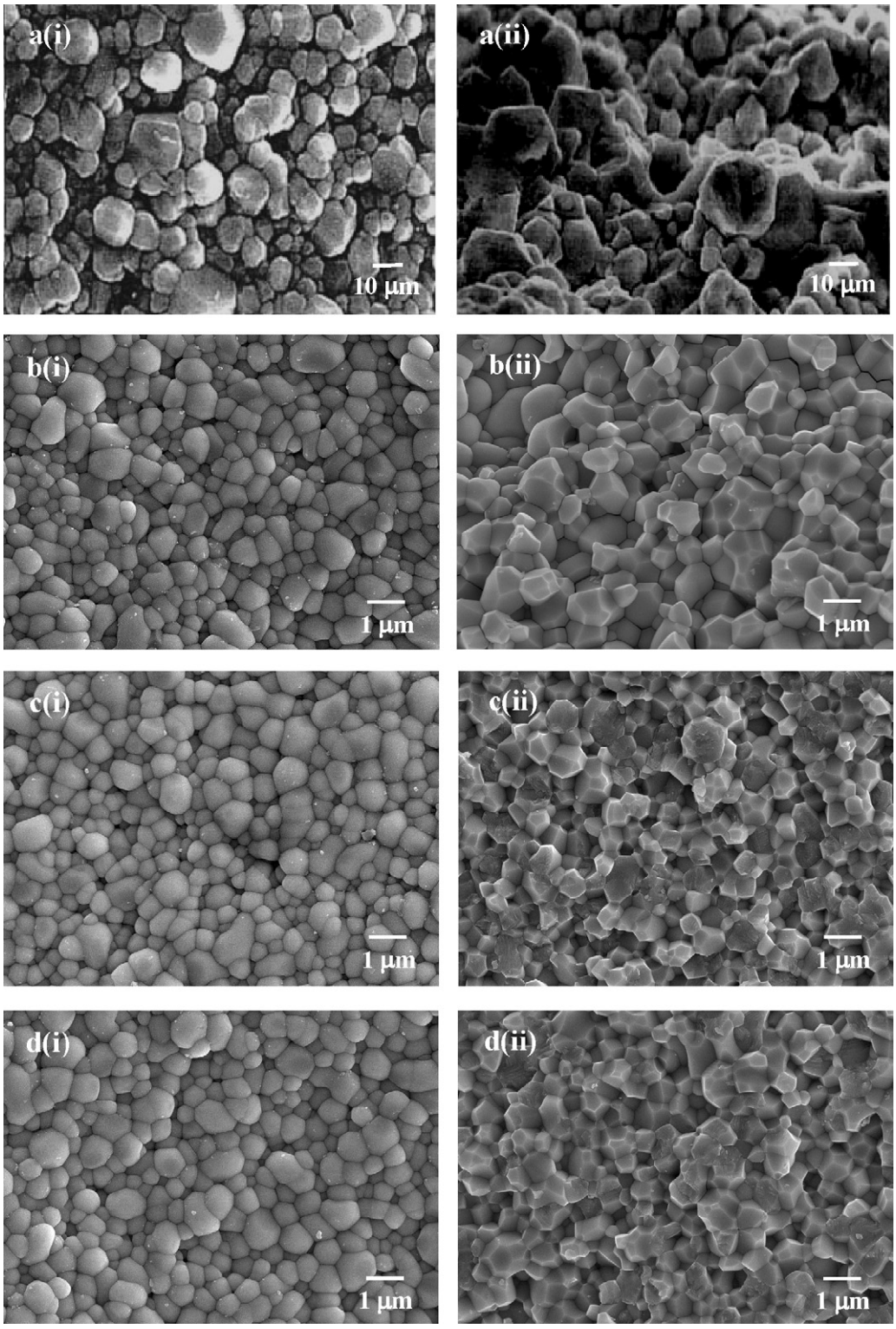

Fig. 3. Natural (i) and fractured (ii) surfaces of (a) monolithic PT and PT/ZnO ceramics with (b) 0.1 wt%, (c) 0.5 wt%, (d) 1 wt%, (e) 3 wt% and (f) 5 wt% of ZnO.

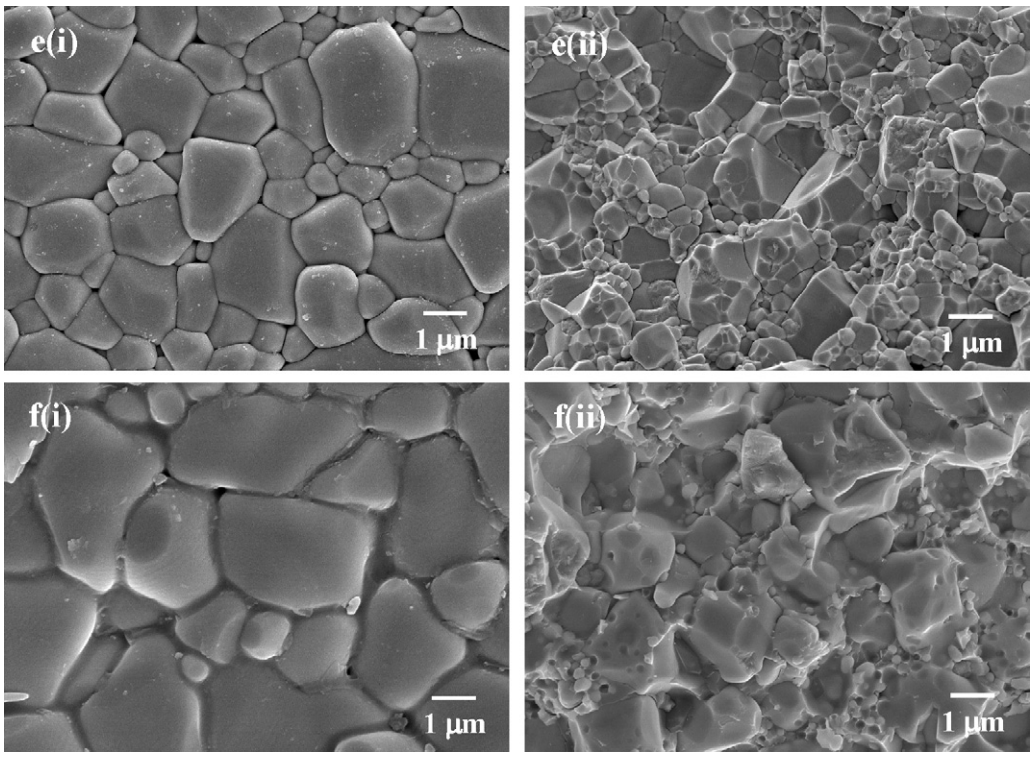

Fig. 3. (*Continued*).

oxygen vacancies accelerated mass transfer and densification – which was observed in other systems [26,27] – was valid in this system. This indicates that ZnO improved the sinterability of PT ceramics. Compared to pure PT ceramics, the composites have a smaller tetragonality factor, indicating a lower internal stress in these nanocomposites [16,17]. These data were estimated through the Cohen method [28]. One explanation for the decrease in tetragonality of the PT/ZnO could be the incorporation of Zn ions into the PT lattice during sintering [29]. Moreover, the results indicated that the addition of Zn^{2+} into the PT phase slightly reduced the lattice dimensions.

Microstructural features – natural (i) and fractured (ii) surfaces – of pure PT ceramics and PT/ZnO composites are displayed in Fig. 3. Pure PT ceramics have spherical grains and poor packing. In contrast, PT/ZnO nanocomposites possess equiaxed grains with good grain-packing. The average grain sizes were found to decrease significantly with increasing content of ZnO up to 3.0 wt%. It seems that ZnO nanowhiskers controlled grain boundary movement and limited grain growth of the PT matrix [17,29]. The samples with 3.0 and 5.0 wt% ZnO – Fig. 3 e(i) and f(i) – show clearly abnormal grain growth. These are important quantitative aspects of liquid-phase sintered microstructures. Moreover, in the sample with 5.0 wt% ZnO, a pronounced second phase is segregated at the grain boundaries, as shown in Fig. 3 f(i). The presence of these (second-phase) layers could be attributed to a liquid-phase formation during the sintering. Also, this same behavior can be noticed in other ceramic systems [30,31]. Thus, it can be concluded that ZnO acted as a sintering aid.

Generally, the fracture mode of samples with 0.1–1.0 wt% ZnO nanowhiskers was found to be predominantly of an intergranular-type, similar to that of monolithic PT ceramics because clear grain boundaries can be observed. In contrast [32,33], almost clean microstructures with highly uniform, dense, angular grain-packing are observed. On the other hand, with increasing ZnO content (more than 3.0 wt%), the samples have two grain size ranges, as shown in Fig. 3 e(ii) and f(ii). Movement of atoms is driven by differences in curvature between the particles in contact, probably because the particles have irregular shapes caused by milling [34]. Moreover, it is possible that the mass transport between several aggregated particles and the high anisotropy in the grain boundary energies induced the formation of compact polyhedral and irregular grains [34]. This indicates that two mechanisms are involved during sintering. Furthermore, it should be noted that the average grain sizes of all the PT/ZnO nanocomposites are smaller than the critical value of 3 μm [32,35], which gives rise to a volumetric percentage adequate to buffer the anisotropic stress caused by the phase transition [1]. The reduced grain size of the composites is considered to be responsible for the improvement of their mechanical properties [35,36].

Fig. 4 shows variations of dielectric constant and dielectric loss of the samples with different ZnO contents at various temperatures, as measured at 1 MHz. Dielectric constant (ε_r) and dielectric loss ($\tan\delta$) values at room temperature, and ferroelectric–paraelectric phase transition temperatures (T_C) of the samples are listed in Table 2. Generally they all behave as typical, normal ferroelectric materials [1]. A similar trend in dielectric values at T_C was also observed. From Fig. 4 b(i), it is evident that the addition of 0.1 wt% ZnO to PT leads to a drastic increase in dielectric constant. The dielectric constant of the composites then decreases slightly with further ZnO addition up to 1.0 wt%. However, the dielectric constant for all PT/ZnO composites appears to be higher than for pure PT ceramics. The higher dielectric constant of samples with small amounts of ZnO could be attributed mainly to the decrease in porosity. Moreover, it can be seen that with increasing ZnO content, T_C shifted towards lower temperatures. The shift of the phase transformation temperature in these PT/ZnO composites might be due to a relaxation of transformation-induced internal stress by the ZnO nanowhiskers dispersed in the PT matrix.

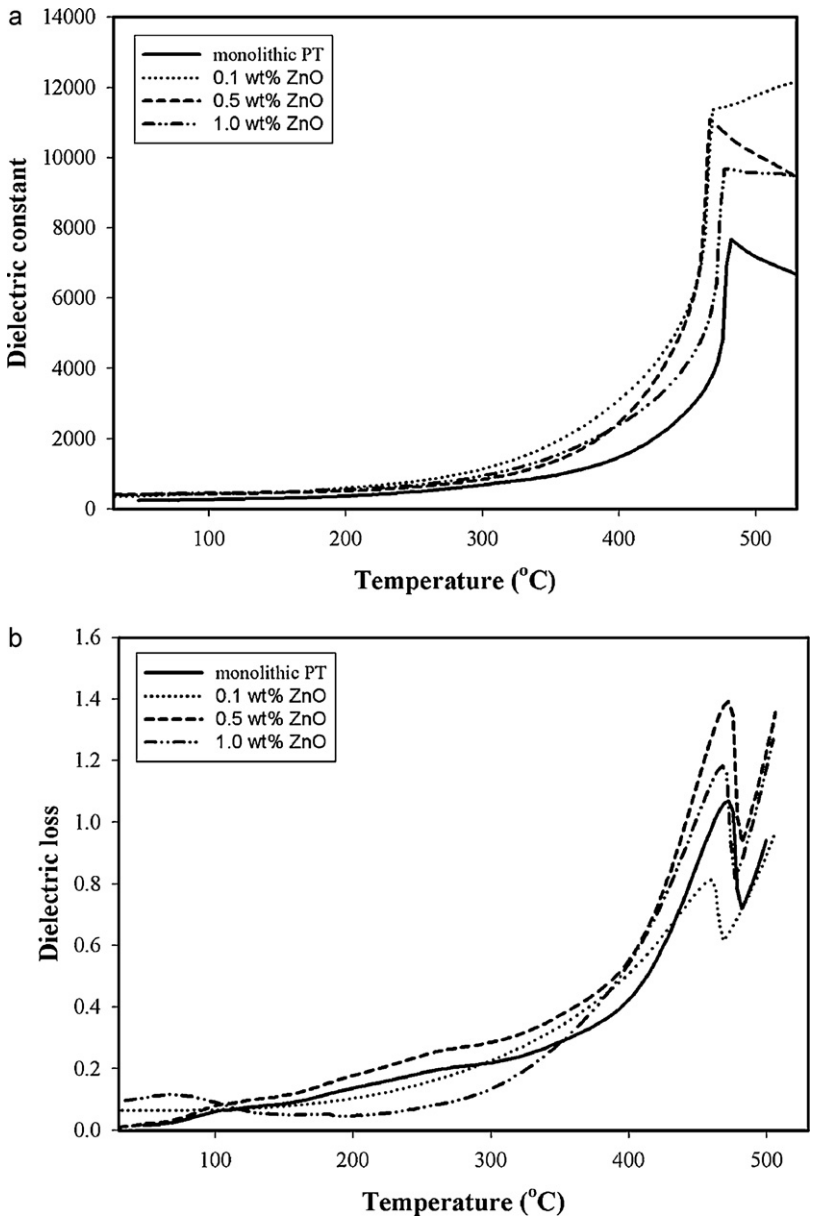

Fig. 4. Variation with temperature of (a) dielectric constant and (b) dielectric loss at 1 MHz of PT/ZnO ceramics with different ZnO contents.

4. Conclusions

$PbTiO_3$/ZnO ceramic composites can be fabricated using a simple and inexpensive solid-state reaction method. The materials had a tetragonal phase for all compositions. Moreover, the addition of ZnO nanowhiskers was found to significantly enhance densification, mechanical and dielectric properties of PT-based ceramics.

Acknowledgements

This work was supported by the Thailand Research Fund (TRF), the Commission on Higher Education (CHE), the National Nanotechnology Center (NANOTEC), and the Faculties of Science of Chiang Mai University and Maejo University. Also acknowledged for additional support are: the Industry/University Cooperative Research Center (I/UCRC) in HDD Component; the Faculty of Engineering, Khon Kaen University; and the National Electronics and Computer Technology Center (NECTEC) of the National Science and Technology Development Agency.

References

[1] A.J. Moulson, J.M. Herbert, Electroceramics, 2nd ed., Wiley, Chichester, 2003.
[2] E.C. Paris, M.F.C. Gurgel, T.M. Boschi, M.R. Joya, P.S. Pizani, A.G. Souza, E.R. Leite, J.A. Varela, E. Longo, J. Alloys Compd. 462 (2008) 157–163.
[3] R. Wongmaneerung, A. Rujiwatra, R. Yimnirun, S. Ananta, J. Alloys Compd. 475 (2009) 473–478.
[4] K. Ramam, M. Lopez, K. Chandramouli, J. Alloys Compd. 488 (2009) 211–216.
[5] C.C.M. Wu, M. Kahn, W. Moy, J. Am. Ceram. Soc. 79 (1996) 809–812.
[6] A.A. Yar, M. Montazerian, H. Abdizadeh, H.R. Baharvandi, J. Alloys Compd. 484 (2009) 400–404.
[7] M.H. Maneshian, M.K. Banerjee, J. Alloys Compd. 493 (2010) 613–618.
[8] S.K. Pandey, O.P. Thakur, D.K. Bhattacharya, C. Prakash, R. Chatterjee, J. Alloys Compd. 468 (2009) 356–359.
[9] Y. Wu, T. Feng, J. Alloys Compd. 491 (2010) 452–455.
[10] J. Yuan, D.W. Wang, H.B. Lin, Q.L. Zhao, D.Q. Zhang, M.S. Cao, J. Alloys Compd. 504 (2010) 123–128.
[11] M. Ipek, S. Zeytin, C. Bindal, J. Alloys Compd. 509 (2011) 486–489.
[12] F.X. Li, X.X. Yi, Z.Q. Cong, D.N. Fang, Mod. Phys. Lett. B 21 (2007) 1605–1610.
[13] J. Cui, G. Dong, Z. Yang, J. Du, J. Alloys Compd. 490 (2010) 353–357.
[14] H.J. Hwang, K. Watari, M. Sando, M. Toriyama, K. Niihara, J. Eur. Ceram. Soc. 19 (1999) 1179–1182.
[15] H.J. Hwang, T. Nagai, T. Ohji, M. Sando, M. Toriyama, K. Niihara, J. Am. Ceram. Soc. 81 (2005) 709–712.
[16] R. Wongmaneerung, R. Yimnirun, S. Ananta, Appl. Phys. A 86 (2007) 249–255.

[17] R. Wongmaneerung, P. Singjai, R. Yimnirun, S. Ananta, J. Alloys Compd. 475 (2009) 456–462.
[18] C. Ionascu, R. Schaller, Mater. Sci. Eng. A 442 (2006) 175–178.
[19] M.S. Cao, W. Zhou, X.L. Shi, Y.J. Chen, Appl. Phys. Lett. 91 (2007) 203110.
[20] S. Choopan, N. Hongsith, S. Tanunchai, T. Chairuangsri, P. Mangkorntong, N. Mangkorntong, J. Cryst. Growth 282 (2005) 365–369.
[21] H. Klug, L. Alexander, X-Ray Diffraction Procedures for Polycrystalline and Amorphous Materials, 2nd ed., Wiley, New York, 1974.
[22] JCPDS-ICDD Card No. 6-452, International Centre for Diffraction Data, Newtown Square, PA, 2000.
[23] S.K. Manik, S.K. Pradhan, Physica E 33 (2006) 69–76.
[24] R. Wongmaneerung, R. Yimnirun, S. Ananta, J. Electroceram. 21 (2007) 798–801.
[25] K. Vanheusden, W.L. Warren, C.H. Seager, D.R. Tallant, J.A. Voigt, B.E. Gnade, J. Appl. Phys. 79 (1996) 7983–7990.
[26] H.J. Hwang, M. Yasuoka, M. Sando, M. Toriyama, K. Niihara, J. Am. Ceram. Soc. 82 (2004) 2417–2422.
[27] P.H. Xiang, X.L. Dong, C.D. Feng, N. Zhong, J.K. Guo, Ceram. Int. 30 (2004) 765–772.
[28] B.D. Cullity, Elements of X-Ray Diffraction, 2nd ed., Addison Wesley, Sydney, 1978, p. 363.
[29] Y. Xu, A. Zangvil, A. Kerber, J. Eur. Ceram. Soc. 17 (1997) 921–928.
[30] M.L. Arefin, F. Raether, D. Dolejš, A. Klimera, Ceram. Int. 35 (2009) 3313–3320.
[31] P. Yongping, L. Yunhe, Y. Wenhu, J. Rare Earths 25 (2007) 167–170.
[32] A. Udomporn, K. Pengpat, S. Ananta, J. Eur. Ceram. Soc. 24 (2004) 185–188.
[33] R. Wongmaneerung, R. Yimnirun, S. Ananta, Appl. Phys. A 86 (2007) 2498–3255.
[34] M.N. Rahaman, Sintering of Ceramics, CRC Press/Taylor and Francis Group, Boca Raton, FL, 2008, pp. 55–106.
[35] L.B. Kong, W. Zhu, O.K. Tan, J. Mater. Sci. Lett. 19 (2000) 1963–1966.
[36] T. Suwannasiri, A. Safari, J. Am. Ceram. Soc. 76 (1993) 3155–3158.